


# Screening and Identification of a Novel Anti-Siglec-15 Human Antibody 3F1 and Relevant Antitumor Activity<sup>S</sup>

Jiaguo Wu, Jingyi Peng, Yangyihua Zhou, Ran Zhang, Zhihong Wang, Naijing Hu, Dingmu Zhang, Guiqi Quan, Yuanyu Wu, Jiannan Feng, Beifen Shen, Jian Zhao, Yan Zhang, Kaiming Yang, and  Longlong Luo

Department of Anatomy, School of Basic Medical Sciences of Dali University, Dali, China (J.W., K.Y.); State Key Laboratory of Toxicology and Medical Countermeasures, Institute of Pharmacology and Toxicology, Beijing, China (J.W., J.P., Y.Zho., Z.W., N.H., D.Z., G.Q., Y.W., J.F., B.S., L.L.); Joint National Laboratory for Antibody Drug Engineering, the First Affiliated Hospital, School of Medicine, Henan University, Kaifeng, China (J.P.); Hunan Normal University School of Medicine, Changsha, China (Y.Zho., R.Z., G.Q.); JOINN Biologics, Co., Ltd, Beijing, China (J.Z.); and Department of Obstetrics and Gynecology, First Medical Center, General Hospital of Chinese PLA, Beijing, China (Y.Zha.)

Received November 30, 2021; accepted June 19, 2022

## ABSTRACT

Sialic acid-binding Ig-like lectin-15 is an important immunosuppressive molecule considered to be a key target in next-generation tumor immunotherapy. In this study, we screened 22 high-affinity antibodies that specifically recognize human Siglec-15 by using a large human phage antibody library, and five representative sequences were selected for further study. The results showed the binding activity of five antibodies to Siglec-15 (EC<sub>50</sub> ranged from 0.02368  $\mu$ g/mL to 0.07949  $\mu$ g/mL), and in two Siglec-15-overexpressed cell lines, three antibodies had the strongest binding activity, so the two clones were discarded for further study. Subsequently, the affinity of three antibodies were measured by bio-layer interferometry technology (5–9  $\times$  10E–09M). As the reported ligands of Siglec-15, the binding activity of Siglec-15 and sialyl-Tn, cluster of differentiation 44, myelin-associated glycoprotein, and leucine-rich repeat-containing protein 4C can be blocked by three of the antibodies. Among these, 3F1 had a competitive advantage. Then, the antibody 3F1 showed an obvious antibody-dependent cell-mediated cytotoxicity effect (EC<sub>50</sub>

was 0.85  $\mu$ g/mL). Further, antibody 3F1 can reverse the inhibitory effect of Siglec-15 on lymphocyte proliferation (especially CD4<sup>+</sup>T and CD8<sup>+</sup>T) and cytokine release Interferon- $\gamma$ . Given the above results, 3F1 was selected as a candidate for the in vivo pharmacodynamics study. In the tumor model of Balb/c Nude mice, 3F1 (10 mg/kg) showed certain antitumor effects [tumor growth inhibition (TGI) was 31.5%], while the combination of 3F1 (5 mg/kg) and Erbitux (5 mg/kg) showed significant antitumor effects (TGI was 48.7%) compared with the PBS group. In conclusion, novel human antibody 3F1 has antitumor activity and is expected to be an innovative candidate drug targeting Siglec-15 for tumor immunotherapy.

## SIGNIFICANCE STATEMENT

Siglec-15 is considered as an important target in the next generation of tumor immunotherapy. 3F1 is expected to be the most promising potential candidate for targeting Siglec-15 for cancer treatment and could provide a reference for the development of antitumor drugs.

## Introduction

In recent years, an important development in tumor immunology is the concept of “immune checkpoints” and the prominent therapeutic effect of targeting specific “immune checkpoint molecules” in the field of antitumor (Alsaab et al., 2017; Chen and

Mellman, 2017; Sharma et al., 2017; Ribas and Wolchok, 2018; Larkin et al., 2019; Vasan et al., 2019). These immune checkpoint molecules exist widely in the tumor microenvironment and lead to adaptive resistance mechanisms of tumor cells against an immune response (Dong et al., 1999; Freeman et al., 2000; Sanmamed and Chen, 2018; Palakurthi et al., 2019; van Dijk et al., 2019). For example, the antibody against B7-H1 or PD-1 blocks the B7-H1/PD-1 pathway (anti-PD therapy for short in this article), which normalizes the immune response in the tumor microenvironment through relieving tumor cells from immune response by effectors T cells, producing favorable tumor treatment results (Dong et al., 2002; Taube et al., 2012; Syn et al., 2017; Kim et al., 2018). In addition to anti-PD therapy,

This research was supported by the National Natural Sciences Foundation of China grant (No. 31771010 and No. 81700122) and Beijing Nova Program (No. Z211100002121020).

The authors declare that there are no conflicts of interest or personal relationships that could have appeared to influence the work reported in this paper.

J.W., J.P., and Y.Zho. contributed equally to this work.

dx.doi.org/10.1124/molpharm.121.000470.

<sup>S</sup> This article has supplemental material available at [molpharm.aspetjournals.org](http://molpharm.aspetjournals.org).

**ABBREVIATIONS:** ABBREVIATIONS: ADCC, antibody-dependent cell-mediated cytotoxicity; CD44, cluster of differentiation 44; FACS, fluorescence activated cell sorting; HRP, horseradish peroxidase; KD, dissociation constant; LRRC4C, leucine-rich repeat-containing protein 4C; MAG, myelin-associated glycoprotein; MFI, median fluorescence intensity; OD, optical density; PBMC, peripheral blood mononuclear cell; Siglec, sialic acid-binding Ig-like lectin; TAM, tumor-associated macrophage; TMB, Trimethylbenzene; 2-YT, Tryptone Yeast Extract.

the Siglec receptor family has been recognized as an important target for tumor immunotherapy in recent years (Angata et al., 2007; Crocker et al., 2007; Pillai et al., 2012; Chang and Nizet, 2014; Macauley et al., 2014).

Siglecs belong to I-type lectin family. To date, 14 different mammalian Siglecs have been identified that mediate cell-to-cell or pathogen interactions by identifying sugar chains containing sialic acid (Chik et al., 2014), which plays an important regulatory role in innate and adaptive immunity (Pillai et al., 2012; Kang et al., 2020). The Siglec family is divided into two classes, one of which has conserved sequences, including sialoadhesin (Siglec-1), CD22 (Siglec-2), MAG (Siglec-4), and Siglec-15, which show low sequence homology. The other class of Siglecs has variable sequences associated with CD33 (Bornhöft et al., 2018). The Siglec-15 gene encodes a short extracellular binding domain, the extracellular binding domain of Siglec-15 contains a variable region of immunoglobulin (IgV) and a type 2 homeostasis region (IgC2), which shares more than 30% similarity to the B7 gene family (Li et al., 2020). It was previously proved that the combination of Siglec-15 and B7-H1 has a synergistic effect in an animal model of colorectal cancer (Wang et al., 2019). Studies have shown that Siglec-15 is highly expressed in liver, lung, thyroid, and bladder cancer tissues and in tumor-associated macrophages (TAMs), whereas low expression in most normal tissues and immune cells suggests that targeting Siglec-15 drugs may have fewer side effects (Angata et al., 2007; Takamiya et al., 2013; Kizuka et al., 2017). Human Siglec-15 has been reported as acting as a TAM receptor that recognizes sialyl-Tn antigen, also known as Neu5Ac $\alpha$ 2, 6GalNAc, that is a sialylated glycan and commonly expressed in tumors. Crosslinking Siglec-15 on TAMs by sialyl-Tn expressed on cancer cells induces TGF- $\beta$  secretion via the DAP12-SYK pathway, which affects tumor progression. In addition to sialyl-Tn, CD44, MAG, and LRRC4C also act as ligands on Siglec-15, mediating immune escape in tumor microenvironments. Wang et al. (2019) studies have shown that deleting Siglec-15 in mice or administering antibodies against Siglec-15 have significant antitumor effects, transforming the immunosuppressive tumor microenvironment into proinflammatory and antitumor immunophenotypes. Furthermore, Siglec-15 and PD-1 gene expression is mutually exclusive, indicating anti-Siglec-15 therapy may also be suitable for treating patients who do not respond to anti-PD therapy. Overall, Siglec-15 may become the next-generation “promising immunotherapy target” after PD-1-targeted therapy.

In this study, we aimed at screening and identifying the potential therapeutic antibodies against Siglec-15. A novel human antibody 3F1, with antitumor activity, was obtained through a series of verifications and biologic evaluation. We will make great efforts to promote preclinical and clinical research of candidate antibodies, hoping to provide more opportunities for targeting Siglec-15 in the field of antitumor. Our experiments were not designed to test a prespecified statistical null hypothesis; therefore, our study should be considered as exploratory.

## Materials and Methods

**Reagents.** Siglec-15-His protein (Cat. No. CW37), Siglec-15/Fc protein (Cat. No. CY14), mouse-Siglec-15 protein (Cat. No. CW71), cynomolgus-Siglec-15 protein (Cat. No. CW70), CD44 protein (Cat. No. C579), and MAG protein (Cat. No. C897) were purchased from Novoprotein corporation (Beijing, China); LRRC4C expression plasmid

(Cat. No. RC207363) was purchased from OriGene Technology Co., Ltd. (Maryland); Poly (ethylene glycol) was purchased from ChemicalBooSk corporation (Beijing, China) (Cat. No. 25322-68-3); M13K07 helper phage (Cat. No. N0315S) was purchased from New England Biolabs, Inc.; jetPRIME transfection reagent (Cat. No. 114-01) was purchased from Univ Biotechnology Co., Ltd. (Shanghai, China); OPM-293 CD05 medium (Cat. No. 81075-001) was purchased from Shanghai OPM Biosciences Co., Ltd. (Shanghai, China); streptavidin-horseradish peroxidase (Cat. No. S911) was purchased from Thermo Fisher Scientific Co., Ltd. (Massachusetts); APC-labeled streptomycin (streptavidin-APC, Cat. No. SA10-10), APC-conjugated goat anti-human IgG Fc (Cat. No. 410712), and HRP-conjugated goat anti-human IgG Fc (Cat. No. 398006) was purchased from Agilent (California). ELISA MAX Standard Set Human kit (IFN- $\gamma$ ) (Cat. No. 430101) was purchased from Biotegend (California); Trimethylbenzene (TMB) color developing solution (Cat. No. CW0050S) was purchased from Beijing ComWin Biotech Co., Ltd. (Beijing, China); coating solution: 0.1M sodium carbonate-sodium bicarbonate buffer (pH 9.6; sodium carbonate Cat. No. 10018960; sodium bicarbonate Cat. No. 1001891922) was purchased from Sinopharm Chemical Reagent Co., Ltd. (Beijing, China); PBS (Cat. No. G4200-500ML) was purchased from Servicebio corporation (Wuhan, China); PBST (0.1% Tween 20 added to PBS, Cat. No. 11973-MM05T-H) (Washing immunotubes during phage screening); protein interaction running buffer solution (0.2% Tween 20 added to PBS); anti-M13/HRP was purchased from Sino Biologic Inc. (Beijing, China); 2-Tryptone Yeast Extract (2-YT) medium (tryptone 16 g, yeast extract 10 g, NaCl 5 g, agar powder 15 g, constant volume to 1 L); tryptone (Cat. No. LP0042) and yeast extract (Cat. No. LP0021) were purchased from Shanghai Gensheng Biotechnology Co., Ltd.; agar powder (Cat. No. A8190) was purchased from Solarbio Technology Co., Ltd. (Beijing, China); Fluorescence activated Cell Sorting (FACS) solution (2% serum in PBS), destaining solution (ethanol 250 mL, 75 mL glacial acetic acid, pure water diluted to 1000 mL), ONE-Glo Luciferase Assay System (Cat. No. E6110) was purchased from Promega Biotechnology Co., Ltd. (Madison, Wisconsin); Mycoplasma PCR Detection Kit (Cat. No. C0301S) was purchased from Beyotime Biotechnology (Shanghai, China). Anti-sialyl-Tn fluorescent antibody (Cat. No. ab115957) was purchased from Abcam (Cambridge, UK); anti-human CD3 antibody (Cat. No. 555916) was purchased from Becton, Dickinson, and Company (Franklin Lake, New Jersey); Erbitux (Cat. No. Ab00279-1.7-BS) were purchased from Biotegend corporation (California); PB513B vector was purchased from System Biosciences corporation (California); pcDNA5/FRT vector was purchased from Thermo Fisher Scientific Co., Ltd. (Massachusetts) (Cat. No. V601020). The natural phage library and antiricin monoclonal antibody MIL50 (in clinical stage) was prepared in and has been preserved in our laboratory.

**Cell Culture.** 293T, MC38, and NCI-H157 cells were from the American Type Culture Collection Center. ADCC Fc $\gamma$ RIIIa (158F) Jurkat Effector Cell Line was purchased from Jenomeditech Biotechnology corporation (Cat. No. GM-C01619). All the cultured cells were tested for mycoplasma contamination using the Mycoplasma PCR Detection Kit, and the cells without mycoplasma contamination were used for further studies. 293T and MC38 cells were cultured in Dulbecco's modified Eagle's medium containing 10% FBS. NCI-H157 cells were cultured in RPMI 1640 medium containing 10% FBS. ADCC Fc $\gamma$ RIIIa (158F) Jurkat Effector Cell Line was cultured in medium containing 10% FBS, 0.75  $\mu$ g/mL puromycin, and 3.5  $\mu$ g/mL Blastincidin. The above cells were placed in an incubator at constant temperature and humidity (Thermo, Waltham, Massachusetts,) at 37°C with 5% CO $_2$ . All cells were cultured for more than three generations, and the cells were in logarithmic growth phase before the experiment.

**Plasmid Construction, Protein Expression, and Stable Strain Construction.** Human Siglec-15 sequence information was obtained from the Uniprot website (Q6ZMC9). According to the sequence information, the full-length Siglec-15 and the Ig-like V-type sequence were intercepted (the detailed amino acid sequence is shown in Supplemental Table 1). To achieve the membrane expression of the Ig-like V-type sequence, the C-terminal of the Ig-like V-type sequence was inserted into the platelet-derived

growth factor receptors transmembrane region to achieve membrane expression. The above gene sequence was synthesized and cloned into commercial vector PB513B using specific restriction endonuclease sites and termed as PB513B-S15 or PB513B-S15-D1. The PB513B-S15 plasmid was transfected into 293T cells and NCI-H157 cells, while the PB513B-S15-D1 plasmid was transfected into 293T cells. Stable strains expressing Siglec-15 or Siglec-15-D1 on the cell surface were obtained by puromycin pressurization. The corresponding stable cell lines were named 293T (S15<sup>+</sup>), 293T (S15-D1<sup>+</sup>), and NCI-H157 (S15<sup>+</sup>), respectively. At the same time, Siglec-15-D1 linked with human IgG1 Fc was cloned into commercial vector pcDNA5/FRT, and Siglec-15-D1/Fc fusion protein was prepared using the 293T expression system.

**Phage Selection for Human Antibody Against Siglec-15.** Ten micrograms of Siglec-15-His protein was dissolved in 500  $\mu$ L of PBS and added to the immunotube at 4°C overnight. After overnight coated, discarded the remaining liquid in the immunotube, added 500  $\mu$ L of 4% skim milk powder formulated with PBS to each immunotube to seal the exposed site for 1 hour at room temperature, simultaneously,  $5 \times 10^{12}$  natural phage libraries were diluted in 4% skim milk and sealed at room temperature for 1 hour. Five hundred microliters of the blocked phage solution was added and incubated at room temperature for 1 hour. The immunotube was washed with PBST (0.1% Tween 20 in PBS) 25–30 times to remove unbound and nonspecifically bound phage, and glycine-hydrochloric acid (100 mmol/L, pH 1.7) was used to elute the specifically bound phage and neutralized with Tris base (pH 8.0). The washed phage was added to TG1 in logarithmic growth phase and incubated at 37°C for 0.5 hour. After centrifugation, the pellet was spread on 2-YT solid medium (containing 100  $\mu$ g/mL ampicillin and 2% glucose) and cultivated overnight. The number of clones were then counted, and the input/output ratio was calculated. Fifty percent glycerol was used to scrape the bacteria on the plate, and the next round of screening was carried out. The harvested bacterial solution from the first round was added to the 2-YT liquid medium (containing 100  $\mu$ g/mL ampicillin and 2% glucose) in proportion. The bacterial solution was cultured at 37°C, 220 r/min for 2.5 hours until the optical density<sub>600</sub> (OD<sub>600</sub>) absorbance of the culture medium was between 0.8 and 1, then the M13K07 helper phage was added and incubated at 37°C for 0.5 hours. The supernatant was discarded after centrifugation, and the precipitates were resuspended in 2-YT liquid medium (containing 100  $\mu$ g/mL ampicillin and 80  $\mu$ g/mL kanamycin) and cultured at 28°C, 220 r/min for 16–22 hours. The phage was precipitated with PEG8000, and the precipitate was resuspended in 20% glycerol and stored at –80°C. Following this, the third round of screening was carried out according to the above method. After three rounds of screening, single clones were randomly picked from bacterial culture plate and cultured in a deep-well plate for 4 hours. Subsequently, 100  $\mu$ L of supernatant was aspirated from each well for subsequent sequencing.  $5 \times 10^{10}$  M13K07 was added to each well of the deep plate and incubated at 37°C for 0.5 hours. Following centrifugation, the supernatant was discarded and 1 mL 2-YT medium (containing 100  $\mu$ g/mL ampicillin and 80  $\mu$ g/mL kanamycin) was added to resuspend it and cultured at 28°C, 220 r/min for 16–22 hours. The centrifuged supernatant was collected for subsequent experiments.

**Preliminary Identification of Phage-Positive Clones via ELISA Assay.** The first domain of Siglec-15 is the ligand binding domain. To initially determine the binding epitope of positive clones, the Siglec-15/Fc protein and Siglec-15-D1/Fc protein were diluted in coating solution to a final concentration of 1  $\mu$ g/mL and added to the ELISA plate at a volume of 100  $\mu$ L per well, then placed at 4°C overnight. The coating solution was washed off, and the exposure site was sealed with 4% skim milk at 37°C for 1 hour. The supernatant collected after culturing at 28°C, 220 r/min for 16–22 hours was centrifuged again at 1800 r/min at 4°C for 15 minutes and added 100  $\mu$ L per well to the enzyme-linked plate and placed at 37°C for 1 hour. After washing, anti-M13/HRP was added and placed at room temperature for 45 minutes. A color reaction was carried out by adding 100  $\mu$ L TMB substrate in each hole, and the reaction was completed with 2N H<sub>2</sub>SO<sub>4</sub>. The results were read in OD<sub>450</sub> light

absorption assay using an enzyme-labeled instrument (Molecular Devices, Silicon Valley).

**Antibody Expression and Identification.** The antibody sequence obtained from the screening was fused with the Fc of human IgG1 in the form of ScFv (single-chain variable fragment)-Fc and cloned into the commercial eukaryotic expression vector PB513B. The plasmid was extracted with a large-scale plasmid kit. jetPRIME transfection reagent was used to transfect the antibody expression vector into 293T cells. After transfection for 6 hours, the expression medium OPM-293 CD05 was changed and cultured for 72 hours. The supernatant was collected and purified with a protein A chromatography column. SDS-PAGE and size-exclusion chromatography high performance liquid chromatography were used to identify antibody purity and molecular mass.

**ELISA to Identify the Binding Activity of Selected Antibodies.** Siglec-15-His protein was diluted to 1  $\mu$ g/mL in the coating solution and coated according to 100  $\mu$ L per well in ELISA plate, then placed at 4°C overnight. The coating solution was washed off, and the exposure site was sealed with 4% skim milk at 37°C for 1 hour to prevent nonspecific binding. The antibody samples were diluted to 15  $\mu$ g/mL and then diluted four times to obtain eight concentration points. The above diluted samples were added to the plate and placed at 37°C for 1 hour. After washing, secondary antibody (HRP-conjugated goat anti-human IgG Fc) diluted with 1:6000 was added to react for 45 minutes at room temperature. The color reaction was carried out by adding 100  $\mu$ L TMB substrate in each hole, and the reaction was completed with 2N H<sub>2</sub>SO<sub>4</sub>. The results were read using OD<sub>450</sub> light absorption assay using an enzyme-labeled instrument. The experiments were repeated three times under this experimental condition.

**ELISA to Identify Crossreactivity of Selected Antibody.** Human Siglec-15, mouse Siglec-15, cynomolgus Siglec-15, Siglec-2, Siglec-7, Siglec-8, Siglec-9, PD-L1, CD24, CD38, CD47, IL-2RA, IL-4R, IL-17A, and IL-22 protein were diluted with His-tagged to 1  $\mu$ g/mL in the coating solution and placed at 4°C overnight. The coating solution was washed off, and the exposure site was sealed with 4% skim milk at 37°C for 1 hour to prevent nonspecific binding. The antibody samples were diluted to the concentration of 2  $\mu$ g/mL, and 100  $\mu$ L per well was added to the plate to react at 37°C for 1 hour. After washing, secondary antibody (HRP-conjugated goat anti-human IgG Fc) diluted with 1:6000 was added to react for 45 minutes at room temperature. The color reaction was carried out by adding 100  $\mu$ L TMB substrate in each hole, and the reaction was completed with 2N H<sub>2</sub>SO<sub>4</sub>. The results were read in OD<sub>450</sub> light absorption assay using an enzyme-labeled instrument. The experiments were repeated three times under these experimental conditions.

**Affinity Determination.** Bio-layer interferometry technology was used to detect antibody affinity. The Siglec-15-His proteins were fixed on the Ni-NTA chip, and the antibody samples were serially diluted with protein interaction running buffer solution (500 nM, 166.7 nM, 55.6 nM, 18.5 nM, 6.17 nM, 2.05 nM, 0.68 nM). The association reaction time was set at 180 s, and the dissociation reaction time was set at 180 s. After the reaction, the reaction was regenerated in 500 mM imidazole for 5 seconds and in protein interaction running buffer solution for 5 seconds. The regeneration-infiltration step was repeated three times. Data analysis 7.0 software was used to analyze the affinity of antibody samples. Imported the raw data automatically generated by the computer into the Data analysis 7.0 software, analyzed the kinetic method, obtained the binding dissociation constant, and drew the kinetic curve. The experiments were repeated three times under this experimental condition.

**Determining the Binding Activity of Antibody by Flow Cytometry.** Cultivated 293T (S15<sup>+</sup>), 293T (S15-D1<sup>+</sup>) stable strains that expressed Siglec-15 and Siglec-15-D1 on the cell membrane surface. When in the logarithmic growth phase, the cells were digested with 0.25% trypsin and washed with FACS solution. The cells were counted at  $5 \times 10^5$  cells per tube. The anti-Siglec-15 antibody was diluted to 15  $\mu$ g/mL and then diluted three times to obtain seven concentration gradients, of which 100  $\mu$ L was added to the corresponding cells and incubated at 4°C for 30 minutes. Secondary antibodies (APC-conjugated

goat anti-human IgG Fc) were added and incubated at 4°C for 30 minutes. After washing twice, BD FACSAria II flow cytometry was used to measure fluorescence. Flowjo 10.4 software was used to analyze the results. The experiments were repeated three times under this experimental condition.

**Determination of Antibody Blocking Activity by ELISA.** CD44 and MAG protein were diluted to 1 µg/mL in the coating solution, and the ELISA plate was coated with 100 µL per well and placed at 4°C overnight. The coating solution was washed off, and the exposure site was sealed with 4% skim milk at 37°C for 1 hour to prevent nonspecific binding. Fifty microliters of Siglec-15-Fc-biotin (the final concentration was 5 µg/mL) and antibody (the final concentration was 50 µg/mL) were added to the corresponding plate and placed at 37°C for 1 hour. After washing, the secondary antibody (streptavidin-HRP) diluted with 1:6000 was added and left to react for 45 minutes at room temperature. The color reaction was carried out by adding 100 µL TMB substrate to each hole, and the reaction was completed using 2N H<sub>2</sub>SO<sub>4</sub>. The results were read in OD<sub>450</sub> light absorption assay with an enzyme-labeled instrument. The experiments were repeated three times under these experimental conditions.

**Determination of the Blocking Activity of Antibodies by Flow Cytometry.** The LRRC4C expression plasmid was transiently transfected into 293T cells in the logarithmic growth phase and cultured for 48 hours. The cells were then digested with 0.25% trypsin and resuspended to  $5 \times 10^5$  cells per tube with FACS solution. Following this, 50 µL of each Siglec-15-Fc-biotin (the final concentration was 5 µg/mL) and antibody (the final concentration was 100 µg/mL) were added to the tube. Siglec-15-Fc-biotin (the final concentration was 5 µg/mL) without antibody was set as the positive control, and all reactions were incubated at 4°C for 30 minutes. Finally, 100 µL secondary antibody (streptavidin-APC) diluted at 1:3000 was added and incubated at 4°C for 30 minutes. After washing twice, flow cytometry was used to measure fluorescence. The activity of antibody blocking the interaction between Siglec-15 and LRRC4C was analyzed. The experiments were repeated three times under this experimental condition.

NCI-H157 cells were cultured when the cells were in the logarithmic growth phase, and the cells were digested with 0.25% trypsin. The cells were washed with FACS solution and resuspended to  $5 \times 10^5$  cells per tube, and the commercial antibody against sialyl-Tn fluorescent antibody was added to detect sialyl-Tn antigen expression on the tumor cells. At the same time, 50 µL of each Siglec-15-Fc-biotin (the final concentration was 5 µg/mL) and antibody (the final concentration was 100 µg/mL) were added to the corresponding tubes. Siglec-15-Fc-biotin (the final concentration was 5 µg/mL) without antibody was set as the positive control, and streptavidin-APC was set as the secondary antibody control, and all reactions were incubated at 4°C for 30 minutes. Each well had 100 µL secondary antibody (streptavidin-APC) added to dilute to 1:3000 and was incubated at 4°C for 30 minutes. After washing twice, flow cytometry was used to measure fluorescence. The antibody activity blocking the interaction between Siglec-15 and sialyl-Tn was analyzed. The experiments were repeated three times under this experimental condition.

**ADCC Activity.** ADCC Fc $\gamma$ RIIIa (158F) Jurkat effector cell line was cultivated as effector cells, and 293T (S15<sup>+</sup>) was used as target cells. When the cells were in the logarithmic growth phase, the cells were digested from the culture flask and culture dish and resuspended in RPMI 1640 medium containing 10% FBS, and the cell viability was checked ( $\geq 95\%$ ). Following this step, effector cells and target cells were added to a flat-bottomed 96-well plate at a concentration of 1:6, i.e., the final concentration of effector cells was  $2.5 \times 10^4$  cells per well, and the final concentration of target cells was  $1.25 \times 10^5$  cells per well, then 50 µL was added to the corresponding plate. Diluted the three candidate antibodies of 1B4, 2A12 and 3F1 and the irrelevant antibody control (MLI50) to 300 µg/mL, fivefold dilution, eight gradients, 50 µL were added into the plate, i.e., the final concentration of antibodies were 100 µg/mL, 20 µg/mL, 4 µg/mL, 0.8 µg/mL, 0.16 µg/mL, 0.032 µg/mL, 0.0064 µg/mL, and 0.00128 µg/mL, three replicates wells

for each sample. The 96-well plate was placed in a cell incubator at 37°C with 5% CO<sub>2</sub> for 6 hours. One hundred microliters of ONE-Glo reagent was added to each well and left to react for 2 minutes in the dark. After the cells were completely lysed, the luciferase value was tested on the GloMax NAVIGATOR machine. The ADCC activity of the antibody samples were calculated. The experiments were repeated three times under this experimental condition.

**Lymphocyte Proliferation.** Peripheral blood mononuclear cells (PBMCs) were isolated from heparinized blood of five healthy donors using ficoll-hypaque density gradient centrifugation. Anti-human CD3 was diluted with PBS to 0.1 µg/mL, and 100 µL was added to each well in a flat-bottomed 96-well plate, which was placed at 4°C overnight. PBMC was isolated using density gradient centrifugation. The separated PBMC were resuspended in 1 mL PBS at a concentration of  $1 \times 10^7$  cells per mL. CFSE was added to the cells at a final concentration of 5 µM and incubated for 10 minutes at room temperature. One-fourth volume of FBS was added, and the samples were centrifuged at 1200 rpm for 4 minutes to discard the supernatant. The cells were resuspended in RPMI 1640 medium containing 10% FBS, and the cell concentration was adjusted to  $2.5 \times 10^6$ . One hundred microliters per hole was added to the middle 60 wells of the 96-well plate. At the same time, 50 µL of each Siglec-15-Fc (15 µg/mL; i.e., a final concentration of 5 µg/mL) protein or diluted Siglec-15 antibody (150 µg/mL, fivefold dilution, three gradients; i.e., final concentrations of 50 µg/mL, 10 µg/mL, and 2 µg/mL) were added to the wells. The 96-well plate was placed in a cell incubator at 37°C with 5% CO<sub>2</sub> for 72 hours. The cells were collected for flow cytometry analysis. To further determine the proliferation of T-cell subsets, anti-CD4 and CD8 fluorescent antibodies were added to the cells, and they were incubated at 4°C for 30 minutes. After washing twice with FACS solution, the labeled cells were analyzed by flow cytometry. The experiments were repeated three times under this experimental condition.

**Lymphocyte Activity.** Anti-human CD3 antibody was diluted with PBS to 0.1 µg/mL, and 100 µL was added to each well of a flat-bottomed 96-well plate, which was placed at 4°C overnight. The liquid in the orifice was aspirated, and PBMC cells were isolated using the method in Lymphocyte Proliferation. All steps followed this method except for the CFSE staining step. The corresponding PBMC Siglec-15/Fc and diluted antibody samples were added to the plate. The 96-well plate was placed in a cell incubator at 37°C with 5% CO<sub>2</sub> for 72 hours. The cell supernatant was harvested, and ELISA MAX Standard Set Human kit (IFN- $\gamma$ ) was used to measure the levels of IFN- $\gamma$ . The experiments were repeated three times under this experimental condition.

**Animal Experiment.** Six- to 8-week-old female Balb/c Nude mice were purchased from Beijing Vital River Laboratory Animal Technology Co., Ltd and placed in the specific pathogen-free environment for 1 week. During this animal experiment, we observed animal ethics during the research according to the "3R" principles of replacement, reduction, and refinement; the use or treatment of the mice was in strict agreement with the guidelines for the care and use of research animals and was approved by the Animal Ethics Committee of the Beijing Institute of Pharmacology and Toxicology. NCI-H157 (S15<sup>+</sup>) was subcutaneously inoculated at a density of  $3 \times 10^6$  cells per mouse. When the tumor volume reached approximately 100 mm<sup>3</sup>, the mice were labeled with ear nails and arranged in descending order according to the tumor size, and the mice were divided into four groups with six mice in each group according to the random number table. PBS was used as the negative control group, 3F1 (10 mg/kg) or Erbitux (10 mg/kg) was used as the monotherapy group, and 3F1 (5 mg/kg) combined with Erbitux (5 mg/kg) was used as the combined therapy group. The drug was administered intraperitoneally twice per week, and the tumor size and mice body weights were monitored during the administration process. The tumor volume was calculated according to the following equation: tumor volume (mm<sup>3</sup>) =  $1/2 \times \text{length} \times \text{width}^2$ . After the treatment was completed, the mice were anesthetized, and the tumors were dissected, weighed, and photographed. After the assay, the mice were sacrificed using

anesthesia with ketamine followed by cervical dislocation; we then used deep freezing to confirm death.

**Statistical Analysis.** Statistical analysis was performed using GraphPad Prism 8 software (San Diego, California). Data were shown as mean plus or minus S.D. Sample sizes were fixed before data were observed, and all in vitro experiments were replicated three times under the same experimental conditions.  $EC_{50}$  values were calculated using a nonlinear regression analysis. The statistical significance of tumor volume and tumor weight between groups at the end of treatment was determined by one-way ANOVA with Tukey test. The intergroup comparison in the Tukey testing after ANOVA had been specified before data were observed. Data were considered statistically significant for  $P$  values lower than 0.05. A post hoc analysis had been chosen in the intergroup comparisons. Three intergroup comparisons had been done, including one low  $P$  value and two high  $P$  values. Based on the exploratory character of our study, calculated  $P$  values should not be interpreted as hypothesis testing but only as descriptive.

## Results

**Phage Panning for Human-Specific Siglec-15 Antibody.** In previous work, the laboratory established a large human phage antibody library and screened multiple therapeutic antibody candidates for specific antigens (Hu et al., 2021b). The same technique was used to screen Siglec-15 antibodies in this study. In the process of phage panning, the input and output of phages were recorded, and the ratio of input and output was calculated (Table 1). According to the input/output ratio histogram in Fig. 1A, the input/output ratio showed a decreasing trend after three rounds of screening, indicating that the phages that specifically recognized Siglec-15 antigen were effectively enriched. The phage supernatant was prepared from five 96 deep well plates randomly selected from the titrated culture dishes produced by the third round of screening. Twenty-two clones with  $OD_{450}$  greater than 1.5 were selected by ELISA for detecting the binding activity of phage supernatant to Siglec-15/Fc. According to literature (Angata et al., 2007), the 143-position arginine ( $R^{143}$ ) existed in the first domain of Siglec-15 is highly conserved in the Siglec family and is known as “essential arginine,” which plays an important role in the recognition of glycan. The mutation in  $R^{143}$  almost caused complete loss of Siglec-15/glycan binding activity. The first domain of Siglec-15 is a functional and important domain, so we constructed the Siglec-15-D1/Fc protein for functional screening and epitope verification. As shown in Fig. 1B, apart from two clones, 1D1 and 4H3, which did not bind to Siglec-15-D1/Fc, the remaining 20 clones could either bind to Siglec-15-D1/Fc or Siglec-15/Fc. Finally, five sets of antibody sequences were identified in 22 selected positive clones (one: 1A11, 1D4, 1F10, 3E5, 5D2; two: 1B4, 1C1, 1F2, 3D12, 5D6; three: 1D8, 2A12, 3A3, 3C8, 4C1; four: 1E7, 3F1, 2C9, 3F3, 2C9, 3F3, 4E4; five: 1D1, 4H3).

TABLE 1

Phage selection for Siglec-15 and related input, output, and input/output ratios

Screening Round	Input	Output	Input/Output
1 <sup>st</sup> round	5.00E+12	9.00E+04	5.56E+07
2 <sup>nd</sup> round	2.00E+12	7.22E+04	2.77E+07
3 <sup>rd</sup> round	1.00E+12	6.02E+06	1.66E+05

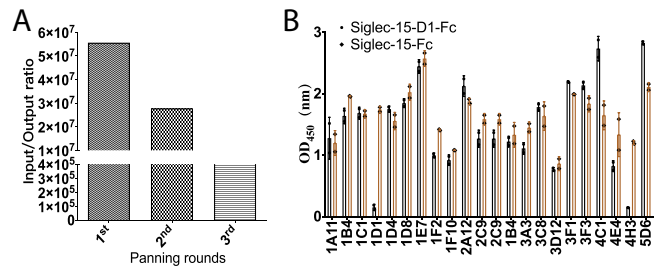


**Fig. 1.** Screening and preparation of fully human antibody library specifically targeting Siglec-15. (A) Histogram of input/output ratio. After three rounds of screening, the input/output ratio showed a decreasing trend, indicating that the positive clones recognizing Siglec-15 had been effectively enriched. (B) The binding activity of 22 clones to Siglec-15/Fc and Siglec-15-D1/Fc as measured by ELISA.

Therefore, 1D4, 1B4, 2A12, 3F1, and 1D1 were selected for the following functional verification.

**Antibody Expression and Binding Activity Verification.** The candidate antibodies were prepared in the single-chain variable fragment (ScFv)-IgG1 format, for which variable region of heavy chain and variable region of light chain were linked with flexible linker ( $G4S$ )<sub>3</sub>, fused to the IgG1 Fc, and expressed by 293T expression system, then purified by protein A. The protein was characterized by SDS-PAGE and size-exclusion chromatography high performance liquid chromatography. Fig. 2A showed the SDS electropherogram of the antibody using Coomassie-stained gel under reducing and nonreducing conditions. The results showed that the molecular mass of these five antibody proteins were 55 kDa and 130 kDa under reducing and nonreducing conditions, respectively, corresponding to the theoretical values of the antibody sequence. Supplemental Fig. 1 showed that 1B4 has a tendency to form aggregates whereas the other four antibodies appeared as monomers and have purity over 90%. Indirect ELISA was conducted to test crossbinding between different species of Siglec-15 and five candidate antibodies, as shown in Fig. 2B. From the results, 1B4 and 2A12 could bind to human/mouse/cynomolgus Siglec-15 effectively, 1D4 and 3F1 could effectively bind to human/cynomolgus Siglec-15, and 1D1 could only bind to human-Siglec-15, with very weak binding activity to mouse-Siglec-15 and no binding activity to cynomolgus. Furthermore, four human Siglec family member proteins and a variety of human cell membrane or secretory proteins were selected to verify the specificity of the antibodies. Results are shown in Fig. 2C. The five antibodies only bound specifically to Siglec-15 antigen and did not crossbind to other proteins. The binding activity of five candidate antibodies to Siglec-15 was tested by indirect ELISA in Fig. 2D. The results showed that all of the five antibodies were able to recognize Siglec-15, and the binding activity was concentration dependent. According to the fitted four-parameter equation, the values of the antibody binding at half the effective dose were ranked by numeric value as follows: 2A12 ( $EC_{50}$ : 0.02368  $\mu$ g/mL) < 1B4 ( $EC_{50}$ : 0.02440  $\mu$ g/mL) < 3F1 ( $EC_{50}$ : 0.07949  $\mu$ g/mL) < 1D1 ( $EC_{50}$ : 0.2442  $\mu$ g/mL) < 1D4 ( $EC_{50}$ : 0.6847  $\mu$ g/mL). Furthermore, flow cytometry was operated to verify the binding activity of antibodies to the membrane protein of Siglec-15 or Siglec-15-D1 overexpressed on the constructed 293T (S15<sup>+</sup>) or 293T (S15-D1<sup>+</sup>) stable cells. Fig. 2E showed that 1B4, 2A12, and 3F1 had the strongest binding activity to Siglec-15, and Siglec-15-D1 was overexpressed on the cell surface; however, the binding of 1D4 and 1D1 was



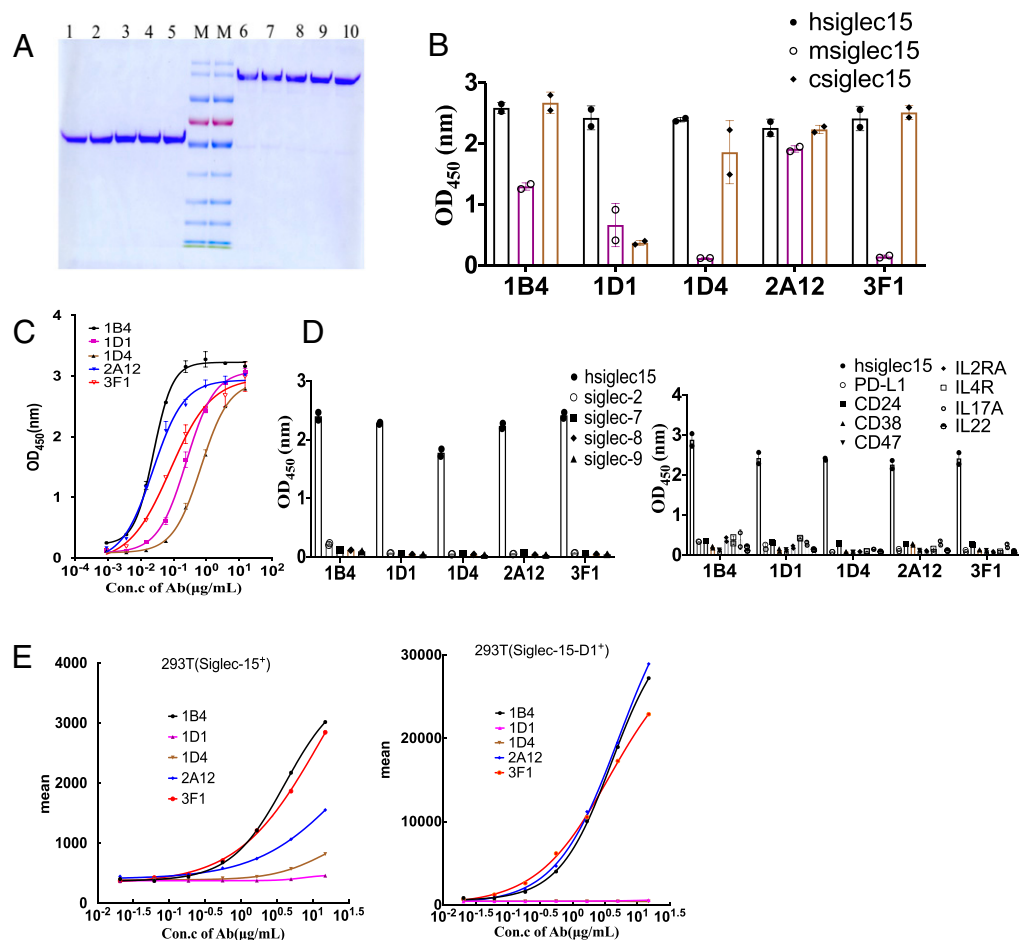


**Fig. 2.** Antibody expression and binding activity verification. (A) SDS electropherogram of candidate antibodies under reducing and nonreducing conditions (bands respectively represent 10 kDa, 17 kDa, 26 kDa, 34 kDa, 43 kDa, 55 kDa, 72 kDa, 95 kDa, 130 kDa, and 180 kDa). One to five are for SDS electrophoresis under reducing conditions, and 6–10 are for SDS electrophoresis under nonreducing conditions of 1B4, 1D1, 1D4, 2A12, and 3F1. As shown in the diagram, the purity of all the proteins is more than 95%, and the molecular masses were 55 kDa and 130 kDa under reducing or nonreducing conditions, respectively. M, protein marker. (B) The indirect ELISA method was used to test crossbinding of five candidate antibodies with different species of Siglec-15. (C) Indirect ELISA was used to determine the binding of the candidate antibodies to four human Siglec family member proteins and eight human cell membrane proteins or secreted proteins. (D) Indirect ELISA was used to verify the binding activity of five candidate antibodies to Siglec-15, and the binding activity was concentration dependent. (E) Flow cytometry was used to verify the binding activity of candidate antibodies to 293T (S15<sup>+</sup>) and 293T (S15-D1<sup>+</sup>).

weak, and the membrane protein is closer to the conformation of natural protein, so the 1D4 and 1D1 clones were discarded for further study. Finally, the affinity of three candidate antibodies were measured by bio-layer interferometry technology. The affinity data were listed in Table 2 and are ranked as follows: 2A12 [dissociation constant (KD):  $5.23 \times 10E-09$ ] < 1B4 (KD:  $9.17 \times 10E-09$ ) < 3F1 (KD:  $1.08 \times 10E-08$ ). The specific association/dissociation fitting diagram is shown in Supplemental Fig. 2.

**The Blocking Activity of Antibody Candidates Against Siglec-15 and Its Ligand.** It has been reported that Siglec-15 has four known ligands: CD44, MAG, sialyl-Tn, and LRRC4C. Flow cytometry were used to detect whether the anti-sialyl-Tn antibody could bind to the 293T cell line that highly expresses LRRC4C; the results showed that the anti-sialyl-Tn antibody could not bind to these cells (Supplemental Fig. 3A). In addition, we also verified that anti-sialyl-Tn antibodies could not bind to CD44 and MAG using biofilm interference technology. Therefore, we believe that the binding of Siglec-15 to CD44, MAG, and LRRC4C may be independent of sialyl-Tn (Supplemental Fig. 3B).

Therefore, the selected antibodies that block Siglec-15 from binding to its ligands have therapeutic potential. To investigate the blocking activity of the antibodies, the CD44 and MAG proteins purchased were coated on the ELISA plate, and antibodies were incubated with Siglec-15-biotin saturation. The saturation concentration of Siglec-15-biotin was verified to be 5 ug/ml in advance. In the statistical analysis, the differences between the antibodies group and the control group were compared respectively to verify that the antibodies have blocking activity, and statistical analyses between antibody groups were performed to compare the difference between the antibodies. Fig. 3A shows three candidate

**TABLE 2**  
Determination of affinity between antibody and Siglec-15 by bio-layer interferometry

Sample ID	KD (M)	Kon (1/ms)	Kdis (1/s)	Full R <sup>02</sup>
1B4	9.17E-09	3.52E+04	3.23E-04	0.999582
2A12	5.23E-09	1.09E+05	5.70E-04	0.997448
3F1	1.08E-08	1.12E+05	1.21E-03	0.960395

antibodies that could compete for binding activity between Siglec-15 and CD44 at a specific concentration, and the corresponding competitive ability was as follows: 3F1 (inhibition rate: 70.04%) > 1B4 (inhibition rate: 54.48%) > 2A12 (inhibition rate: 23.72%). Fig. 3B shows three candidate antibodies that have similar competitive trends for Siglec-15 and MAG, and their corresponding competitive abilities were as follows: 3F1 (inhibition rate: 89.64%) > 2A12 (inhibition rate: 75.18%) > 1B4 (inhibition rate: 45.30%). Since both sialyl-Tn and LRRC4C are membrane receptor molecules, flow cytometry was used to verify the blocking activity of the antibodies. Human non-small-cell lung adenocarcinoma cell line NCI-H157 highly expressed sialyl-Tn antigen on cell membrane surface was used and verified by anti-sialyl-Tn fluorescent antibody (Supplemental Fig. 3C). The blocking activity of three candidate antibodies was shown in Fig. 3C. The interaction of Siglec-15 with the sialyl-Tn antigen could be effectively competed for by the three candidate antibodies at a given concentration. Raw flow results are shown in Supplemental Fig. 3D. Finally, transient transfection of LRRC4C plasmid into 293T cells and transient expression of LRRC4C on the cell membrane was used for flow cytometry analysis. Fig. 3D shows that all three antibody candidates could compete effectively for the interaction between Siglec-15 and LRRC4C at a

given concentration. Raw flow results are shown in Supplemental Fig. 3E.

**Luciferase Reporter Gene Assay for Evaluation of Antibody ADCC Activity.** To evaluate the ADCC activity of antibody, ADCC FcγRIIIa (158F) Jurkat Effector Cell Line was used. Jurkat cells stably express FcγRIIIa (158F) and firefly luciferase driven by NFAT response elements. In theory, the antibody could connect the target cells and effector cells, inducing luciferase expression by activating the NFAT pathway downstream of the effector cells via FcγRIIIa (158F) receptor. In general, the activity of the antibody ADCC can be accessed according to the amount of luciferase expressed. The ADCC activity of the candidate antibodies were verified. Results are shown in Fig. 4A. All of the three candidate antibodies showed an obvious ADCC effect and certain dose dependence. The corresponding EC<sub>50</sub> values were ranked below: 3F1 (EC<sub>50</sub>: 0.85 μg/mL) < 2A12 (EC<sub>50</sub>: 1.31 μg/mL) < 1B4 (EC<sub>50</sub>: 2.90 μg/mL), and the monoclonal antibody MIL50 as an irrelevant antibody control and the results showed it had no ADCC effect.

**Cell Proliferation and Cytokine Release.** It is well known that anti-human CD3 antibodies can stimulate T-cell activation. It has been reported (Ren, 2019; Wang et al., 2019) that Siglec-15 directly inhibits NF-κB/NFAT signaling by binding to unknown receptors on T-cell surfaces. The secretion of IL-10 inhibits the proliferation of T cells and the production of cytokines, thus inhibiting antitumor immunity and promoting tumor growth. In vitro, Siglec-15, independent of macrophages or IL-10, directly inhibits the proliferation and activation of T cells. To verify whether the samples had the same trend among different people, we took blood samples from three volunteers and set up three replicate wells under the same experimental conditions. In this study, anti-human CD3 antibody was used to stimulate T-cell proliferation and cytokine release (IFN-γ). Siglec-15/Fc was added to inhibit T-cell stimulation by anti-human CD3 antibody. Candidate antibodies were added to study the effect of antibodies on reversing the effects of Siglec-15 on T-cell proliferation and the cytokine release of lymphocytes. The cell proliferation of the untreated group and the anti-CD3 group was compared, the difference between the anti-CD3 group and the anti-CD3+S15 group, and also compared the differences between anti-CD3+S15 group with antibody group. The purpose was to test whether antibodies against Siglec-15 can effectively reverse the immunosuppressive effect of Siglec-15 on lymphocytes. As shown in Fig. 4B, mean fluorescence intensity (MFI) values can well reflect the proliferation of T cells: the faster the proliferation of T cells, the lower the MFI value. The lymphocytes proliferated more slowly without anti-human CD3 antibody, with the highest average fluorescence intensity. The T cells proliferated significantly when anti-human CD3 antibody was added. Therefore, the corresponding MFI was significantly lower, and the addition of Siglec-15/Fc protein at a specific concentration could inhibit T-cell proliferation, so the corresponding MFI was significantly higher, the addition of 3F1 could significantly decrease the MFI, and the other two antibodies showed a reversed effect (raw flow result is shown in Supplemental Fig. 4), which indicated that 3F1 can effectively reverse the immunosuppression of Siglec-15/Fc on activated T cells, whereas 1B4 and 2A12 did not have this function. Furthermore, specific CD4<sup>+</sup> and CD8<sup>+</sup> T cells were

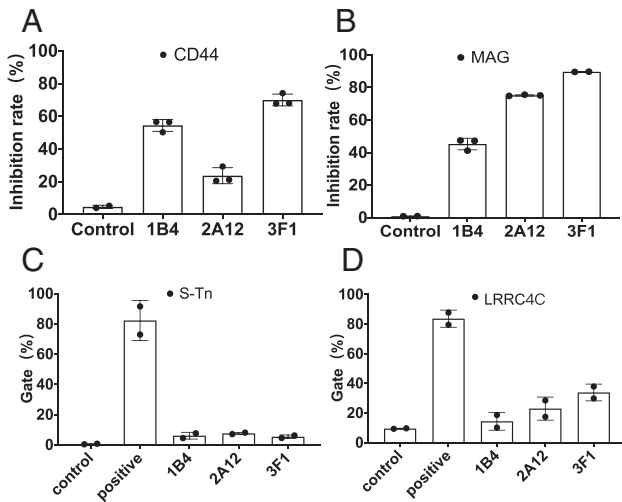


**Fig. 3.** Analysis of blocking activity between candidate antibodies and different ligands of Siglec-15. (A) and (B) showed the inhibition rates of three candidate antibodies against CD44 (A) and MAG (B) with Siglec-15 by ELISA; the calculation formula was  $[1 - (\text{experimental group} - \text{blank control}) / (\text{positive control} - \text{blank control})] \times 100$  (the experimental group added the candidate antibody, and the positive control group had no antibody). Among (A) and (B), all three candidate antibodies could effectively compete with the interaction between Siglec-15, and CD44, MAG at a specific concentration, and 3F1 had the strongest competitive effect. (C) The gate percentage of three candidate antibodies against sialyl-Tn and Siglec-15. Flow cytometry was used to determine the blocking effects of the candidate antibodies and the ligand sialyl-Tn, and the percentage of gate was analyzed. At a specified concentration, all three candidate antibodies effectively competed for interaction between Siglec-15 and sialyl-Tn antigen to the background value. (D) The gate percentage of three candidate antibodies against LRRC4C and Siglec-15. Flow cytometry was used to determine the blocking effect of the candidate antibody and the ligand LRRC4C, and the percentage of gate was analyzed. At a specified concentration, the three candidate antibodies effectively competed with Siglec-15 and LRRC4C. Among (C) and (D), positive group was without antibody, its gate percentage was the highest, and the gate percentage of the antibody group was significantly reduced, reflecting the inhibitory effect of antibody.

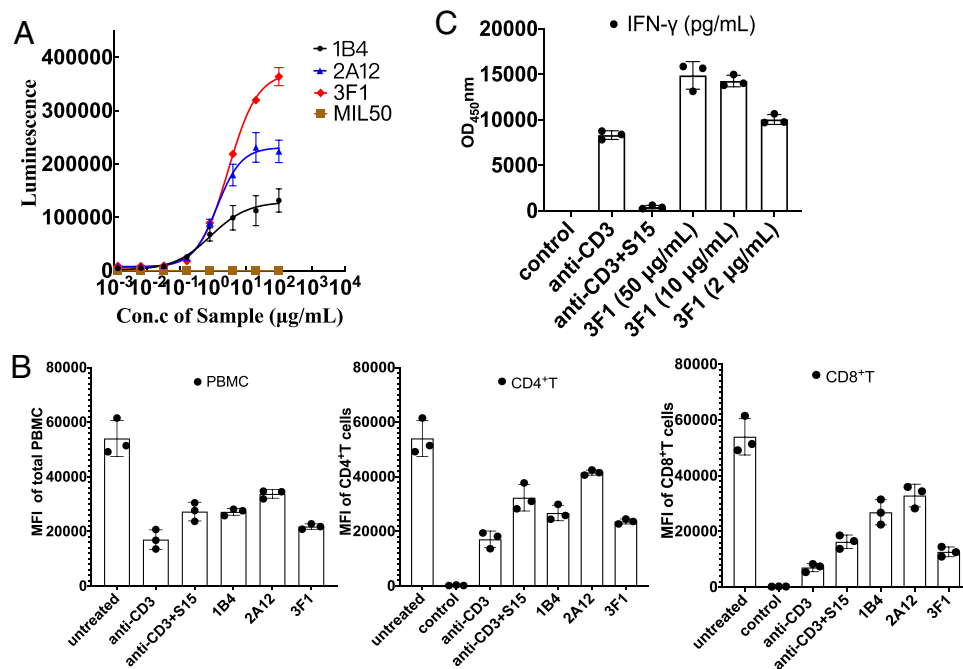


**Fig. 4.** Evaluation of the biologic activity of candidate antibodies in vitro. (A) The ADCC effect of the candidate antibodies was evaluated by detecting the luciferase value at different concentrations. The ADCC effect of the candidate antibody 3F1 was the strongest, the monoclonal antibody MIL50 had no ADCC effect as an irrelevant antibody control. (B) Flow cytometry was used to evaluate the inhibitory effects of the candidate antibodies on reversing the proliferation of human total PBMC mediated by Siglec-15. The candidate antibody 3F1 effectively reversed T-cell proliferation. (C) ELISA was used to detect the influence of the candidate antibodies on the cytokines released into the supernatant of human PBMC. 3F1 was able to increase the levels of IFN- $\gamma$  inhibited by Siglec-15. Adding 50  $\mu$ g/mL, 10  $\mu$ g/mL, and 2  $\mu$ g/mL of 3F1 significantly reversed the level of IFN- $\gamma$  inhibited by Siglec-15/Fc, and the result was concentration-dependent.

labeled with anti-CD4<sup>+</sup> and CD8<sup>+</sup> T fluorescent antibodies, and their proliferation was analyzed. The results show that the results and the above results were consistent. Considering that 3F1 has better competitive activity in vitro (such as Siglec-15 and ligands CD44 and MAG), stronger ADCC activity and a potential stronger reversal effect (3F1 reverses the ability of Siglec-15 to inhibit lymphocyte proliferation), 3F1 was selected as a candidate for further study.

In addition, we further evaluated the reversal of immunosuppression by 3F1 in the lymphocyte cytokine release (IFN- $\gamma$ ) assay. Results are shown in Fig. 4C, where the level of IFN- $\gamma$  was lower without anti-human CD3 antibody, the IFN- $\gamma$  value was significantly increased to a higher level when adding anti-human CD3 antibody, and this could be reversed by Siglec-15/Fc. On this basis, the addition of 3F1 was able to increase the level of IFN- $\gamma$ , and the effect was concentration dependent. This suggests that candidate antibody 3F1 could effectively reverse the immunosuppressive effect of Siglec-15 on lymphocytes.

**Evaluation of Biologic Activity in Vivo.** It was reported that Siglec-15 is expressed at low level in normal human tissue but highly expressed in TAMs and multiple tumors, which have a serious impact on patient prognosis. Thus, Siglec-15 has become a hot target in antitumor immunotherapy. In this study, an overexpressed Siglec-15 tumor cell line was genetically constructed based on NCI-H157, and the tumor cells were inoculated subcutaneously into Nude mice with certain immune deficiencies to form a subcutaneous tumor-bearing model to study the antitumor

activity of the candidate antibody 3F1. Since NCI-H157 itself expresses EGFR molecules (Supplemental Fig. 5), the study tested the therapeutic effects of targeted Siglec-15 and EGFR combinations. In statistical analysis, we separately compared 3F1 (10 mg/kg), Erbitux (10 mg/kg), 3F1 (5 mg/kg), and Erbitux (5 mg/kg) with the PBS group and also compared the differences between three treatment groups. Fig. 5A shows a time-dependent growth curve of tumor size. The results show that, compared with the PBS control group, 3F1 (10 mg/kg) or commercial anti-EGFR antibody Erbitux (10 mg/kg) could inhibit tumor growth. The combination of 3F1 (5 mg/kg) and Erbitux (5 mg/kg) showed a significant antitumor effect. Furthermore, compared with the PBS group, the tumor growth inhibition rates using Erbitux, 3F1 monotherapy, 3F1 and Erbitux combined therapy were 13.9%, 31.5%, and 48.7% respectively. Fig. 5B shows time-dependent mice weight. The results show that the NCI-H157 tumor cells were malignant, and the mice weight in the PBS, 3F1, and Erbitux groups decreased significantly (11.44%, 8.12%, and 7.78%, respectively). An increase was only seen in the combined therapy group (4.64%). Due to animal welfare concerns, the trial was terminated on day 14 of treatment. Fig. 5C shows the weight of the tumor peeled off at the end of the experiment, and the results showed that compared with PBS control group, the 3F1 and Erbitux monotherapy groups had lower tumor weight at the end of the experiment, whereas in the combined therapy group, a significantly lower tumor weight was observed. Fig. 5D shows the tumor photos at the end of experiment. These results indicate that 3F1 has certain



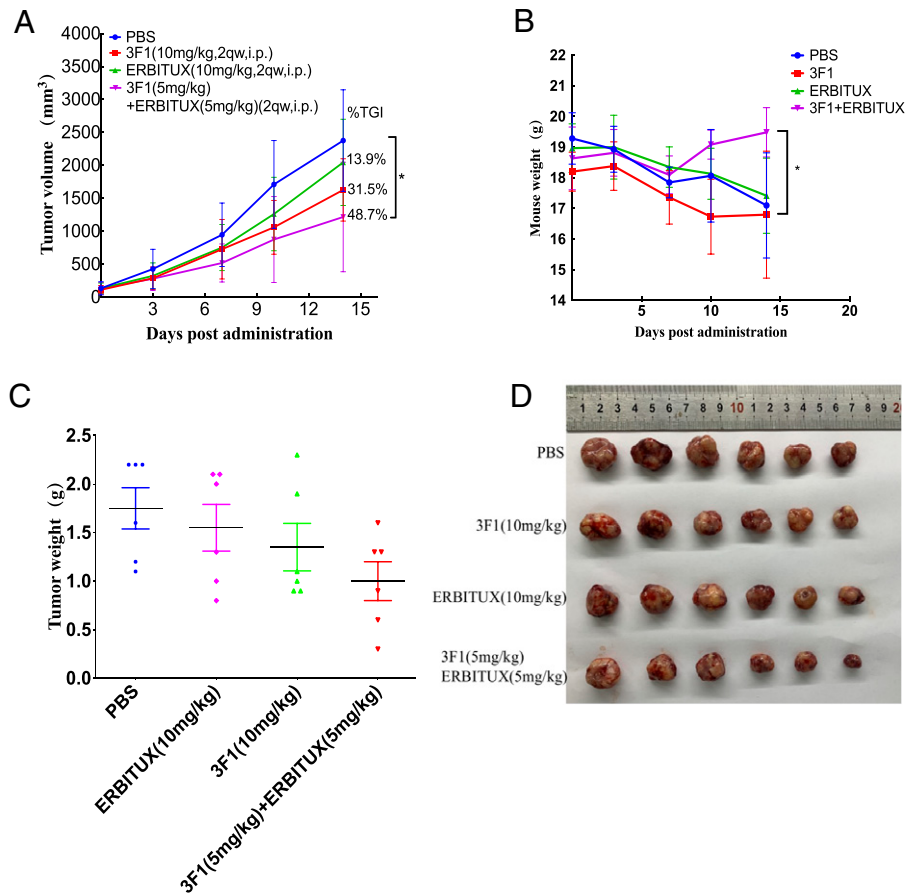


**Fig. 5.** Evaluation of the biologic activity of candidate antibodies in vivo. The last time point data of tumor size, mouse weight, and stripped tumor weight were calculated by one-way ANOVA with Tukey test. 3F1 monotherapy, 3F1 monotherapy, 3F1, and Erbitux combined therapy compared with PBS control group, respectively. (A) The growth curve of tumor size with different drug groups over time; compared with the PBS control group, 3F1 monotherapy (10 mg/kg) and Erbitux monotherapy (10 mg/kg) had a definite antitumor effect ( $P > 0.05$ ). The combined treatment group of 3F1 (5 mg/kg) and Erbitux (5 mg/kg) combined therapy showed an obvious antitumor effect ( $P < 0.05$ ) ( $n = 6$ ). (B) The percentage increase/decrease in body weight of mice over time. Apart from the combined treatment group, which showed a slight increase in mice weight, all other groups showed a significant reduction in mice weight ( $P > 0.05$ ). (C) The tumor peeled off at the end of the experiment, and the 3F1 and Erbitux combined therapy group had a significantly lower tumor weight. (D) Photograph of detached tumor in each group. The last time point data of tumor size, mouse weight, and stripped tumor weight were calculated by one-way ANOVA with Tukey test. (\* $P < 0.05$ ; \*\* $P < 0.01$ ; \*\*\* $P < 0.001$ ; \*\*\*\* $P < 0.0001$ ).  $P < 0.05$  was considered statistically significant.

antitumor activity in mice and obvious antitumor activity when combined with Erbitux. The above results indicate that 3F1 could be used as a candidate drug targeting Siglec-15 for antitumor therapy.

## Discussion

In recent years, immunotherapy, especially immune checkpoint blockade, has been widely used in the clinical treatment of malignant tumors (Hanahan and Weinberg, 2011; Pardoll, 2012; Rosenberg et al., 2016; Ribas and Wolchok, 2018; Wei et al., 2018). Multiple studies have shown (Wang et al., 2019; Quirino et al., 2021) that Siglec-15 is less expressed in normal tissues and overexpressed in the tumor microenvironment of many types of cancer and has an immunosuppressive function. This means that Siglec-15 may be a broad-spectrum target with fewer side effects. Recent studies have shown that Siglec-15 plays an important role in regulating the tumor microenvironment and promoting tumor immunosuppression in two main ways. One

is by preferentially binding to the structure of sialyl-Tn (Briard et al., 2018), which is commonly expressed in tumors and may induce TGF- $\beta$  secretion via the intracellular DAP12-Syk signaling pathway of TAMs (Ishida-Kitagawa et al., 2012; Takamiya et al., 2013). Syk is mediated by a variety of intermediate kinases, such as AKT (Yi et al., 2014), PKC (Takada and Aggarwal, 2004; Aggarwal and Pittenger, 2005), ERK (Eliopoulos et al., 2006; Parsa et al., 2008), etc. A large number of studies have shown that TGF- $\beta$  is an important cancer-promoting cytokine in the middle and late stages of cancer (Shi and Massagué, 2003; Meulmeester and Ten Dijke, 2011; Matsushita et al., 2012; Martini et al., 2014; Ahn et al., 2015). TGF- $\beta$  can inhibit immune cells in the tumor microenvironment and can promote the formation of tumor-associated fibroblasts and epithelial-mesenchymal transition, ultimately promoting tumor proliferation and metastasis. It can also do this through the expression of Siglec-15 on TAMs or tumor cells, which binds to an unknown receptor on the T-cell surface (as yet unknown) to inhibit CD8<sup>+</sup> T-cell proliferation (Wang et al., 2019; Murugesan et al., 2021).

A large number of experiments have shown that Siglec-15 has potent immunosuppressive effects in animal tumor models, but the role of Siglec-15 in human tumors and the antitumor effect of blocking Siglec-15 have not been exactly confirmed. Liu et al. (2020) showed that in Siglec-15<sup>+</sup> renal clear cell carcinomas, miR-7109-3p controls the cell surface abundance of Siglec-15 by up-regulating LINC00973, which is involved in cancer immunosuppression. Furthermore, recent studies have demonstrated that Siglec-15 plays an immunomodulatory role in lung adenocarcinoma and bladder cancer and that Siglec-15 may be an important prognostic biomarker (Li et al., 2020; Hu et al., 2021a). Wang et al. (2019) pointed out that Siglec-15 differs from the escape route of PD-1/PD-L1 and that Siglec-15 does not overlap with the expression of PD-1/PD-L1 (Kamoun et al., 2020). This suggests that anti-Siglec-15 inhibitors may be an effective alternative to anti-PD therapy. Phase I clinical trials of anti-Siglec-15 monoclonal antibody NC318 also demonstrated a response in patients with non-small-cell lung carcinoma who did not respond to PD-1 blockers. Currently, clinical trials on NC318 in the treatment of head and neck cancer and triple-negative breast cancer are continuing. As a result, Siglec-15 is expected to become the next major immune checkpoint to benefit some cancer patients who do not respond to current immunotherapy drugs.

Phage display technology is the insertion of DNA sequences of foreign proteins or peptides into the phage capsid protein structure gene at the appropriate location, allowing the foreign gene to be expressed along with capsid protein expression while a biologic technique in which foreign proteins are displayed on the surface of a phage as the phage is reassembled. Phage display, which plays an important role in the directed evolution of enzymes and in the selection of peptides and antibodies, was awarded the Nobel Chemistry Prize in 2018 (<https://www.nobelprize.org/prizes/chemistry/2018/summary/>). In this study, a total of five high-affinity antibodies for Siglec-15 were screened from a human phage antibody library with large capacity constructed in the laboratory. These five candidate antibodies have good binding ability to the antigen, and the affinity constant reaches the nM level. Three strains of antibody (1B4, 2A12, and 3F1) were selected by antigen binding and ligand blocking experiments in vitro. Among these, 3F1 showed better competitive activity in vitro (such as Siglec-15 and ligands CD44 and MAG), stronger ADCC activity, and potential stronger reversal effect. Therefore, 3F1 was selected as a candidate for the in vivo pharmacodynamics study. The results showed that 10 mg/kg of 3F1 had a certain antitumor effect compared with the PBS control group, whereas the combination of 5 mg/kg of 3F1 and 5 mg/kg of Erbitux significantly inhibited tumor growth. In addition, there was no significant weight loss in mice in the combined therapy group. The tumor volume in the combined therapy group was generally smaller than that of other groups, which indicates that the combined therapy group had the strongest antitumor activity. In summary, 3F1 is expected to be a candidate drug for targeting Siglec-15. However, this animal model has some shortcomings. Balb/c Nude mice lacking T cells were not able to be used to evaluate the effect of Siglec-15 on T and B cells. Anti-Siglec-15 monotherapy or combination therapy is more likely to work through antibody Fc effects (such as ADCC, CDC, and ADCP) or through macrophage activation-related pathways.

In conclusion, this study has identified novel anti-Siglec-15 antibody candidate molecule 3F1, which has been tested and shown to have excellent in vitro biologic activity. At the same

time, therapy or combined therapy offers a certain level of in vivo antitumor activity. 3F1 is expected to be the most promising potential candidate for targeting Siglec-15 for cancer treatment.

#### Acknowledgment

The authors thank Springer Nature Group (<https://authorservices.springernature.com/>) for editing a draft of this manuscript.

#### Authorship Contributions

*Participated in research design:* Y.Zho., J.Z., K.Y., L.L.

*Conducted experiments:* J.W, J.P., Y.Zho., R.Z.

*Contributed new reagents or analytical tools:* J.W, J.P., Y.Zho.

*Performed data analysis:* J.W., Z.W., N.H., D.Z., G.Q., Y.W.

*Wrote or contributed to the writing of the manuscript:* J.F., B.S., J.Z., Y.Zha., K.Y., L.L.

#### References

- Aggarwal S and Pittenger MF (2005) Human mesenchymal stem cells modulate allogeneic immune cell responses. *Blood* **105**:1815–1822.
- Ahn YH, Hong SO, Kim JH, Noh KH, Song KH, Lee YH, Jeon JH, Kim DW, Seo JH, and Kim TW (2015) The siRNA cocktail targeting interleukin 10 receptor and transforming growth factor- $\beta$  receptor on dendritic cells potentiates tumour antigen-specific CD8(+) T cell immunity. *Clin Exp Immunol* **181**:164–178.
- Alsaab HO, Sau S, Alzhrani R, Tatiparti K, Bhise K, Kashaw SK, and Iyer AK (2017) PD-1 and PD-L1 Checkpoint Signaling Inhibition for Cancer Immunotherapy: Mechanism, Combinations, and Clinical Outcome. *Front Pharmacol* **8**:561.
- Angata T, Tabuchi Y, Nakamura K, and Nakamura M (2007) Siglec-15: an immune system Siglec conserved throughout vertebrate evolution. *Glycobiology* **17**:838–846.
- Bornhöft KF, Goldammer T, Rebl A, and Galuska SP (2018) Siglecs: A journey through the evolution of sialic acid-binding immunoglobulin-type lectins. *Dev Comp Immunol* **86**:219–231.
- Briard JG, Jiang H, Moremen KW, Macauley MS, and Wu P (2018) Cell-based glycan arrays for probing glycan-glycan binding protein interactions. *Nat Commun* **9**:880.
- Chang YC and Nizet V (2014) The interplay between Siglecs and sialylated pathogens. *Glycobiology* **24**:818–825.
- Chen DS and Mellman I (2017) Elements of cancer immunity and the cancer-immune set point. *Nature* **541**:321–330.
- Chik JH, Zhou J, Moh ES, Christopherson R, Clarke SJ, Molloy MP, and Packer NH (2014) Comprehensive glycomics comparison between colon cancer cell cultures and tumours: implications for biomarker studies. *J Proteomics* **108**:146–162.
- Crocker PR, Paulson JC, and Varki A (2007) Siglecs and their roles in the immune system. *Nat Rev Immunol* **7**:255–266.
- Dong H, Strome SE, Salomao DR, Tamura H, Hirano F, Flies DB, Roche PC, Lu J, Zhu G, Tamada K, et al. (2002) Tumor-associated B7-H1 promotes T-cell apoptosis: a potential mechanism of immune evasion. *Nat Med* **8**:793–800.
- Dong H, Zhu G, Tamada K, and Chen L (1999) B7-H1, a third member of the B7 family, co-stimulates T-cell proliferation and interleukin-10 secretion. *Nat Med* **5**:1365–1369.
- Eliopoulos AG, Das S, and Tschlis PN (2006) The tyrosine kinase Syk regulates TPL2 activation signals. *J Biol Chem* **281**:1371–1380.
- Freeman GJ, Long AJ, Iwai Y, Bourque K, Chernova T, Nishimura H, Fitz LJ, Malenkovich N, Okazaki T, Byrne MC, et al. (2000) Engagement of the PD-1 immunoinhibitory receptor by a novel B7 family member leads to negative regulation of lymphocyte activation. *J Exp Med* **192**:1027–1034.
- Hanahan D and Weinberg RA (2011) Hallmarks of cancer: the next generation. *Cell* **144**:646–674.
- Hu J, Yu A, Othmane B, Qiu D, Li H, Li C, Liu P, Ren W, Chen M, Gong G, et al. (2021a) Siglec15 shapes a non-inflamed tumor microenvironment and predicts the molecular subtype in bladder cancer. *Theranostics* **11**:3089–3108.
- Hu N, Qiao C, Wang J, Wang Z, Li X, Zhou L, Wu J, Zhang D, Feng J, Shen B, et al. (2021b) Identification of a novel protective human monoclonal antibody, LXYS, that targets the key neutralizing epitopes of staphylococcal enterotoxin B. *Biochem Biophys Res Commun* **549**:120–127.
- Ishida-Kitagawa N, Tanaka K, Bao X, Kimura T, Miura T, Kitaoka Y, Hayashi K, Sato M, Maruoka M, Ogawa T, et al. (2012) Siglec-15 protein regulates formation of functional osteoclasts in concert with DNAX-activating protein of 12 kDa (DAP12). *J Biol Chem* **287**:17493–17502.
- Kamoun A, de Reyniès A, Allory Y, Sjö Dahl G, Robertson AG, Seiler R, Hoadley KA, Groeneveld CS, Al-Ahmadie H, Choi W, et al.; Bladder Cancer Molecular Taxonomy Group (2020) A Consensus Molecular Classification of Muscle-invasive Bladder Cancer. *Eur Urol* **77**:420–433.
- Kang FB, Chen W, Wang L, and Zhang YZ (2020) The diverse functions of Siglec-15 in bone remodeling and antitumor responses. *Pharmacol Res* **155**:104728.
- Kim TK, Herbst RS, and Chen L (2018) Defining and Understanding Adaptive Resistance in Cancer Immunotherapy. *Trends Immunol* **39**:624–631.
- Kizuka Y, Nakano M, Yamaguchi Y, Nakajima K, Oka R, Sato K, Ren CT, Hsu TL, Wong CH, and Taniguchi N (2017) An Alkynyl-Fucose Halts Hepatoma Cell Migration and Invasion by Inhibiting GDP-Fucose-Synthesizing Enzyme FX, TSTA3. *Cell Chem Biol* **24**:1467–1478.e5.

- Larkin J, Chiarion-Sileni V, Gonzalez R, Grob JJ, Rutkowski P, Lao CD, Cowey CL, Schadendorf D, Wagstaff J, Dummer R, et al. (2019) Five-Year Survival with Combined Nivolumab and Ipilimumab in Advanced Melanoma. *N Engl J Med* **381**:1535–1546.
- Li B, Zhang B, Wang X, Zeng Z, Huang Z, Zhang L, Wei F, Ren X, and Yang L (2020) Expression signature, prognosis value, and immune characteristics of Siglec-15 identified by pan-cancer analysis. *Oncol Immunology* **9**:1807291.
- Liu Y, Li X, Zhang C, Zhang H, and Huang Y (2020) LINC00973 is involved in cancer immune suppression through positive regulation of Siglec-15 in clear-cell renal cell carcinoma. *Cancer Sci* **111**:3693–3704.
- Macauley MS, Crocker PR, and Paulson JC (2014) Siglec-mediated regulation of immune cell function in disease. *Nat Rev Immunol* **14**:653–666.
- Martini M, De Santis MC, Braccini L, Gulluni F, and Hirsch E (2014) PI3K/AKT signaling pathway and cancer: an updated review. *Ann Med* **46**:372–383.
- Matsushita H, Vesely MD, Koboldt DC, Rickert CG, Uppaluri R, Magrini VJ, Arthur CD, White JM, Chen YS, Shea LK, et al. (2012) Cancer exome analysis reveals a T-cell-dependent mechanism of cancer immunoeediting. *Nature* **482**:400–404.
- Meulmeester E and Ten Dijke P (2011) The dynamic roles of TGF- $\beta$  in cancer. *J Pathol* **223**:205–218.
- Murugesan G, Correia VG, Palma AS, Chai W, Li C, Feizi T, Martin E, Laux B, Franz A, Fuchs K, et al. (2021) Siglec-15 recognition of sialoglycans on tumor cell lines can occur independently of sialyl Tn antigen expression. *Glycobiology* **31**:44–54.
- Palakurthi S, Kuraguchi M, Zacharek SJ, Zudaire E, Huang W, Bonal DM, Liu J, Dhaneshwar A, DePeaux K, Gowaski MR, et al. (2019) The Combined Effect of FGFR Inhibition and PD-1 Blockade Promotes Tumor-Intrinsic Induction of Antitumor Immunity. *Cancer Immunol Res* **7**:1457–1471.
- Pardoll DM (2012) The blockade of immune checkpoints in cancer immunotherapy. *Nat Rev Cancer* **12**:252–264.
- Parsa KV, Butchar JP, Rajaram MV, Cremer TJ, and Tridandapani S (2008) The tyrosine kinase Syk promotes phagocytosis of Francisella through the activation of Erk. *Mol Immunol* **45**:3012–3021.
- Pillai S, Netravali IA, Cariappa A, and Mattoo H (2012) Siglecs and immune regulation. *Annu Rev Immunol* **30**:357–392.
- Quirino MWL, Pereira MC, Deodato de Souza MF, Pitta IDR, Da Silva Filho AF, Albuquerque MSS, Albuquerque APB, Martins MR, Pitta MGDR, and Rêgo MJBM (2021) Immunopositivity for Siglec-15 in gastric cancer and its association with clinical and pathological parameters. *Eur J Histochem* **65**:3174.
- Ren X (2019) Immunosuppressive checkpoint Siglec-15: a vital new piece of the cancer immunotherapy jigsaw puzzle. *Cancer Biol Med* **16**:205–210.
- Ribas A and Wolchok JD (2018) Cancer immunotherapy using checkpoint blockade. *Science* **359**:1350–1355.
- Rosenberg JE, Hoffman-Censits J, Powles T, van der Heijden MS, Balar AV, Necchi A, Dawson N, O'Donnell PH, Balmanoukian A, Loriot Y, et al. (2016) Atezolizumab in patients with locally advanced and metastatic urothelial carcinoma who have progressed following treatment with platinum-based chemotherapy: a single-arm, multicentre, phase 2 trial. *Lancet* **387**:1909–1920.
- Sanmamed MF and Chen L (2018) A Paradigm Shift in Cancer Immunotherapy: From Enhancement to Normalization. *Cell* **175**:313–326.
- Sharma P, Retz M, Siefker-Radtke A, Baron A, Necchi A, Bedke J, Plimack ER, Vaena D, Grimm MO, Bracarda S, et al. (2017) Nivolumab in metastatic urothelial carcinoma after platinum therapy (CheckMate 275): a multicentre, single-arm, phase 2 trial. *Lancet Oncol* **18**:312–322.
- Shi Y and Massagué J (2003) Mechanisms of TGF- $\beta$  signaling from cell membrane to the nucleus. *Cell* **113**:685–700.
- Syn NL, Teng MWL, Mok TSK, and Soo RA (2017) De-novo and acquired resistance to immune checkpoint targeting. *Lancet Oncol* **18**:e731–e741.
- Takada Y and Aggarwal BB (2004) TNF activates Syk protein tyrosine kinase leading to TNF-induced MAPK activation, NF- $\kappa$ B activation, and apoptosis. *J Immunol* **173**:1066–1077.
- Takamiya R, Ohtsubo K, Takamatsu S, Taniguchi N, and Angata T (2013) The interaction between Siglec-15 and tumor-associated sialyl-Tn antigen enhances TGF- $\beta$  secretion from monocytes/macrophages through the DAP12-Syk pathway. *Glycobiology* **23**:178–187.
- Taube JM, Anders RA, Young GD, Xu H, Sharma R, McMiller TL, Chen S, Klein AP, Pardoll DM, Topalian SL, et al. (2012) Colocalization of inflammatory response with B7-h1 expression in human melanocytic lesions supports an adaptive resistance mechanism of immune escape. *Sci Transl Med* **4**:127ra37.
- van Dijk N, Funt SA, Blank CU, Powles T, Rosenberg JE, and van der Heijden MS (2019) The Cancer Immunogram as a Framework for Personalized Immunotherapy in Urothelial Cancer. *Eur Urol* **75**:435–444.
- Vasan N, Baselga J, and Hyman DM (2019) A view on drug resistance in cancer. *Nature* **575**:299–309.
- Wang J, Sun J, Liu LN, Flies DB, Nie X, Toki M, Zhang J, Song C, Zarr M, Zhou X, et al. (2019) Siglec-15 as an immune suppressor and potential target for normalization cancer immunotherapy. *Nat Med* **25**:656–666.
- Wei SC, Duffy CR, and Allison JP (2018) Fundamental Mechanisms of Immune Checkpoint Blockade Therapy. *Cancer Discov* **8**:1069–1086.
- Yi YS, Son YJ, Ryou C, Sung GH, Kim JH, and Cho JY (2014) Functional roles of Syk in macrophage-mediated inflammatory responses. *Mediators Inflamm* **2014**:270302.

---

**Address correspondence to:** Longlong Luo, State Key Laboratory of Toxicology and Medical Countermeasures, Beijing Institute of Pharmacology and Toxicology, P. O. Box 130 (3), Taiping Road #27, Beijing 100850, China. E-mail: luolong\_long@126.com; Yan Zhang, Department of Obstetrics and Gynecology, First Medical Center, General Hospital of Chinese PLA. E-mail: 3348929253@qq.com; Kaiming Yang, Department of Anatomy, School of Basic Medical Sciences of Dali University. E-mail: 176501584@qq.com; or Jian Zhao, JOINN Biologics, Co., Ltd, Beijing 101102, China. E-mail: zhaojian@joinnbio.com.cn

---